

Polymer Chemistry

Accepted Manuscript



This is an *Accepted Manuscript*, which has been through the Royal Society of Chemistry peer review process and has been accepted for publication.

Accepted Manuscripts are published online shortly after acceptance, before technical editing, formatting and proof reading. Using this free service, authors can make their results available to the community, in citable form, before we publish the edited article. We will replace this *Accepted Manuscript* with the edited and formatted *Advance Article* as soon as it is available.

You can find more information about *Accepted Manuscripts* in the [Information for Authors](#).

Please note that technical editing may introduce minor changes to the text and/or graphics, which may alter content. The journal's standard [Terms & Conditions](#) and the [Ethical guidelines](#) still apply. In no event shall the Royal Society of Chemistry be held responsible for any errors or omissions in this *Accepted Manuscript* or any consequences arising from the use of any information it contains.

ARTICLE

Patterning of individual *Staphylococcus aureus* bacteria onto photogenerated polymeric surface structures

Cite this: DOI: 10.1039/x0xx00000x

Marta Palacios-Cuesta^a, Aitziber L. Cortajarena^b, Olga García^{a*} and Juan Rodríguez-Hernández^{a*}.Received 00th January 2012,
Accepted 00th January 2012

DOI: 10.1039/x0xx00000x

www.rsc.org/

This manuscript describes the fabrication of bacterial surface arrays by using photolithographic techniques having in addition some particularly interesting features. The methodology employed is based on the crosslinking and degradation processes occurring in polystyrene upon exposure to UV light. As a result of both processes, this approach produced different patterns depending not only on the mask but also depending on the experimental conditions employed. Patterns with nanoscale resolution were formed without the requirement of expensive fine focalization settings. More interestingly, the feasibility of this strategy to incorporate functional groups to modulate the affinity between the bacteria and the surface is demonstrated. In particular, hydrophilic segments, i.e. poly(acrylic acid) that favor the bacterial immobilization were introduced. The strategy employed allowed not only the incorporation of functional groups but also permits to fine tune the amount of hydrophilic functional groups. This unique feature has been used to determine the role of the surface hydrophilicity on the adhesion of *Staphylococcus aureus* (*S. aureus*) onto the different surface patterns. Finally, those surfaces in which both the photodegradation and photocrosslinking occurred produced thin patterns largely below the micrometer that have been employed to prepare arrays of isolated *S. aureus* bacteria. The formation of bacterial arrays of *S. aureus* on the single-cell level has been a challenge since they exhibit a large tendency to grow in clusters. This technology has a great potential for the isolation of single bacteria for diagnosis, and the study of bacteria populations at the single cell level.

Introduction

The immobilization of microorganisms onto solid surfaces has been extensively studied during the last decade. Bacterial cells adhere almost to any kind of abiotic surface that serves to grow and finally form a biofilm¹⁻³. The interest of preparing surfaces with either adherent or repellent properties towards microorganism has received an increasing interest for many different reasons. On the one hand, antifouling surfaces prepared using water repellent polymers or by anchoring antimicrobial compounds may prevent implants from contamination, reducing device-associated infections⁴. On the other hand, surfaces capable to immobilize and remove microorganisms in a controlled manner have been equally explored for a rather broad range of applications ranging from cellular biology, biofilm construction to the elaboration of more sophisticated systems such as biosensors, or biomolecular motors⁵⁻¹².

Whereas studies have been mainly focused on the removal of bacteria from surfaces several groups have been during the last decade interested in the development of surfaces in which the microorganisms are distributed in a controlled manner. Bacterial microarrays on surfaces have the potential to be employed in the diagnostics of different diseases^{13, 14} microbial ecology¹⁵, genotoxin monitoring¹⁶ and environmental monitoring¹⁷ including the

monitoring of heavy metals in the environment¹⁸ or as assays of gene expression¹⁹. Patterned bacterial surfaces have been equally employed for to fabrication of in vitro model systems for fundamental studies of bacterial processes such as quorum sensing^{17, 20-22} and horizontal gene transfer²³⁻²⁵.

Precise immobilization of microorganisms and in particular bacteria onto surfaces have been achieved by using different fabrication approaches such as soft lithography²⁶, microcontact printing using micropatterned stamps^{27, 28} or replication molding^{10-12, 29} or different lithographic approaches including capillary lithography³⁰, electron-beam lithography³¹, dip-pen nanolithography^{10, 32} or photolithography^{33, 34} or onto functional multilayers³⁵, inkjet printing.³⁶

Typically, the above mentioned approaches succeeded in the immobilization of bacteria on micrometer size regions where, rather than isolated, the bacteria appeared to form aggregates.^{29, 37} According to our knowledge, only few examples reported the controlled immobilization of single bacteria.^{7, 38} The immobilization of isolated bacterial cell has been accomplished by using expensive approaches or time-consuming multistep procedures including dip-pen nanolithography⁷, photolithography³⁹ or structural transformation by electrodeposition on patterned substrates.³⁸ Kasas et al.⁴⁰ and later Dufrêne and coworkers⁴¹ employed an alternative

and immobilized single bacterial cells onto Millipore filters with comparable sizes to the dimensions of the cell. In spite of the simple and inexpensive solution the last strategy is limited to the round shape features and the polydispersity of the pores.

Within this background, in this manuscript we describe the formation of different surface patterns by using a photolithographic based technique that do not require the use of high resolution masks or clean rooms to fabricate surface patterns with micrometer and submicrometer resolution. The principle of this approach is based on the use of polystyrene (PS) as a polymer matrix of a blend. Polystyrene may undergo either crosslinking or degradation reactions depending on the UV-light irradiation conditions employed. More interestingly, as will be described in detail, radical diffusion between the exposed-non exposed areas permits to crosslink in this region with submicrometer precision. Moreover, as mentioned by Anselme *et al.*⁴² photolithography has been typically limited to create topographical structures without the modification of the surface chemistry. Our approach allowed us to precise control the chemical functionality by using copolymers as additives in the PS polymer matrix. As will be described, the chemical functionality will favor the bacterial attachment. More precisely, an amphiphilic block copolymer with hydrophilic PAA groups that will enhance the contact with the bacteria was employed.

As a model bacterial strain to be immobilized *S. aureus*, a Gram positive bacteria that causes a broad number of infections in humans, being the leading cause of hospital acquired infections has been selected. In particular methicillin-resistant *S. aureus* (MRSA), a variant resistant to many antibiotics is an emerging threat to public health. *S. aureus* is spherical shaped bacterium (coccus) of about 1 micrometer diameter. *S. aureus* usually grow in grape-like clusters of several individuals⁴³ Therefore, the isolation of individual bacterium for identification and diagnostic purposes is of highly interest.

Experimental section

Polystyrene (PS), Irgacure 651 (IRG 651 - 2,2-dimethoxy-1,2-diphenylethan-1-one) (Ciba®), and the rest of solvents were employed as received. Glasses with 0.15 mm thickness (Menzel-Glaser) were employed as covers to limit the UV-light exposure. As a substrate microscope slides with a 1 mm thickness (Menzel-Glaser) were used The masks used for this study were copper grids typically used for transmission electron microscopy (using masks with different shaped features, composed of lines, hexagonal or squares and with variable pitch from 62 to 12.5µm pitch).

The synthesis of the block copolymers was achieved by either two consecutive controlled radical polymerization steps using ATRP (Polystyrene-*block*-poly(acrylic acid) (PS₂₃-*b*-PAA₁₁) and polystyrene-*b*-poly[poly(ethylene glycol) methyl ether methacrylate] (PS-*b*-PEGMA) or combining the controlled radical polymerization with the ring-opening polymerization of N-carboxyanhydrides (Polystyrene-*b*-poly(L-glutamic acid) (PS-*b*-PGA). For a detailed description on the synthesis the reader is referred to the supporting information.

The ¹H and ¹³C NMR spectra were registered at room temperature in CDCl₃ solution in Varian INOVA-300. Chemical shifts are reported in parts per million (ppm) using as internal reference the peak of the trace of deuterated solvent (δ 7.26). Size exclusion chromatography (SEC) analyses were carried out on chromatographic system (Waters Division Millipore) equipped with a Waters model 410 refractive-index detector. Dimethylformamide (99.9%, Aldrich) containing 0.1% of LiBr, was used as the eluent at a flow rate of 1 mL min⁻¹ at 50 °C. Styragel packed columns (HR2, HR3 and HR4, Waters Division Millipore) were used. Poly(methyl

methacrylate) standards (Polymer Laboratories, Laboratories, Ltd.) between 2.4x10⁶ and 9.7x10² g mol⁻¹ were used to calibrate the columns. The molecular weights were estimated against these poly(methyl methacrylate) standards.

Atomic force microscopy (AFM) measurements were conducted on a Multimode Nanoscope IVa, Digital Instrument/Veeco operated in tapping mode at room temperature under ambient conditions. All the images are height images in which the clearer color corresponds to elevated areas whereas the darker color is related to deeper areas. Elevated areas result upon crosslinking since these areas are not removed upon rinsing. On the contrary, deeper areas correspond either to non-crosslinked or degraded areas.

For the preparation of the thin films a 30 mg mL⁻¹ solution of PS homopolymer in THF was spin coated onto glass covers at 2000 rpm during 1 min. These films were then irradiated under UV spot light irradiation from source Hamamatsu model Lightningcure L8868 provided by an Hg-Xe lamp with 200W power. The incident light intensity was focused on the samples with an optic fiber placed at a constant distance of 5.5 cm with either 50% or 100% of the total intensity of the lamp using a TEM copper grid as a mask, with different size and/or shape. After irradiation the films were rinsed with THF in order to remove both degraded and non-crosslinked polymer.

Bacterial adhesion tests

S. aureus strain RN4220 carrying the plasmid pCN57 for Green fluorescent protein (GFP) expression (generous gift from Iñigo Lasa's Laboratory at Instituto de Agrobiotecnología, UPNA-CSIC-Gobierno de Navarra) was grown overnight at 37°C in Luria-Bertani (LB) media with erythromycin (10 µg/ml). The cells were centrifuged and washed three times in PBS buffer (150 mM NaCl, 50 mM Na-phosphate pH 7.4). The solution was adjusted to a cell concentration that corresponds to an optical density (OD) at 600 nm of 1.0 checked using an UV-VIS Varian Cary 50 spectrophotometer.

The different patterned polymeric surfaces were incubated for periods ranging from 1 to 4 hours with a bacterial suspension at OD = 1.0 in PBS buffer with 0.05 % Tween 20. After incubation the surfaces were washed with PBS three times during 15 minutes.

Bacteria adhesion was monitored by fluorescence microscopy using a Leica DMI-3000-B fluorescence microscope. Images were acquired using different magnifications (x10, x20, x40 and x63) and the corresponding set of filters for imaging green fluorescence and bright field. Also Scanning Transmission Electron Microscopy (STEM) images were taken using a FESEM apparatus HITACHI SU8000. Samples for STEM were previously immersed in Formalin 10% solution neutral buffered (Aldrich), washed first with water and then with water/ethanol solutions in increasing proportion up to 100% ethanol.

Results and discussion

Polystyrene (PS) is among the most extensively employed polymers due to their optical properties (transparency), the possibility to chemically modify its structure and polymerize with a broad amount of monomers or their easy processability. These characteristics have converted this material in a commonly used material among others in many biorelated applications such as in cell adhesion studies⁴⁴, the fabrication of medical devices able to measure the electrical activity of cells⁴⁵ or to improve the hemocompatibility.⁴⁶

PS has been patterned by using different techniques including hot embossing⁴⁷, breath figures⁴⁸⁻⁵⁰, polymer dewetting on chemically patterned substrates^{51, 52}, by using soft-lithography to pattern silicon substrates grafted with polystyrene chains⁵³, by UV-

laser radiation to produce micro-drilling⁴⁵ or by scanning electrochemical microscopy.⁴⁴ In addition, polystyrene can be photocrosslinked/photodegraded by using UV light. The use of this approach has particular advantages. As has been depicted before the use of a single mask allow us to prepare surfaces with variable surface patterns depending on the extent of photocrosslinking/photodegradation. As will be shown, the possibility to pattern at the interface between the exposed and non-exposed areas permits to achieve resolutions largely below the mask employed. Moreover, in contrast to such techniques as hot-embossing, the patterning can be carried out at room temperature so that the use of copolymers based on polystyrene that may degrade upon heating can be employed as additives.

Photocrosslinking has been typically carried out using different materials in order to create structured surfaces with more or less resolution but usually without paying special attention to their functionality⁴². Within this context, our group reported the use functional copolymers having styrene units and comonomers with either hydrophilic or hydrophobic functional groups to vary the surface chemical composition.^{54, 55} In particular a large number of studies evidenced that surface hydrophilicity plays a key role on the protein immobilization and subsequent cell attachment. Herein, we will explore the possibility to modify the surface chemical composition and their role on the bacterial adhesion. For that purpose, in order to promote bacterial attachment on the photogenerated surface patterns an amphiphilic block copolymer was mixed with a polymer matrix (linear polystyrene). Thus, films composed by polystyrene (employed as reference), and an amphiphilic block copolymer (for instance, polystyrene-*block*-poly(acrylic acid) (PS₂₃-*b*-PAA₁₁) or blends of both components (Figure 1) were irradiated in order to produce different surface patterns.

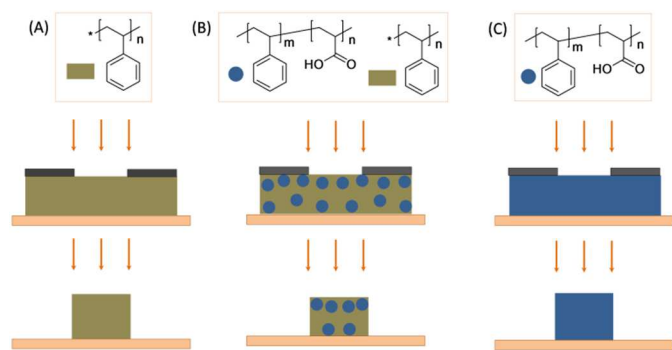


Fig. 1 Homopolymer (PS) and block copolymer (PS₂₃-*b*-PAA₁₁) employed in the preparation of the substrates with photogenerated patterns. (A) Polystyrene (PS), (B) blends of PS and an amphiphilic block copolymer PS₂₃-*b*-PAA₁₁ and (C) films composed exclusively by the amphiphilic block copolymer.

The fabrication of different surface patterns that will serve as platforms to anchor the bacterial cells by UV-irradiation of the polystyrene based surfaces is schematically illustrated in Figure 2. In this particular case a square shaped mask (pitch 25 μm , bar 6 μm and hole 19 μm) has been employed. Equally, the AFM images obtained for each structure and their cross-sectional profiles are included. As depicted in Figure 2(A), at short irradiation times, the regions directly exposed are crosslinked as a consequence of the radical formation and interchain recombination. On the contrary, below the mask the polymer did not receive UV light and, therefore, did not crosslink. Upon rinsing, the polymer below these areas

could be completely removed. In this case, the pattern obtained is the negative of the mask.

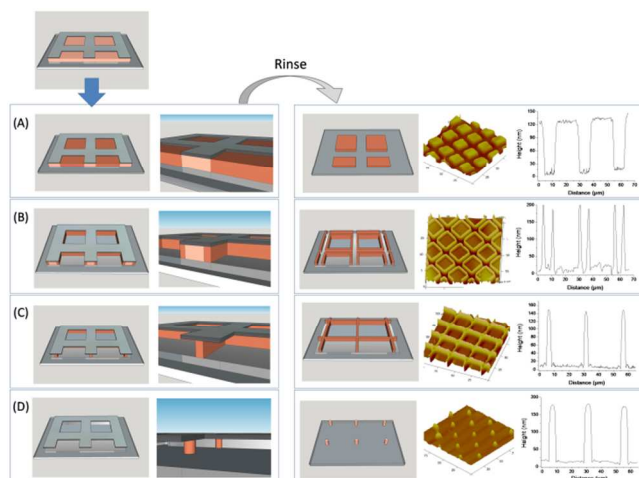


Fig. 2 Structures obtained as a function of the duration of the UV treatment. (A) Square-shaped pattern, (B) closed boxes, (C) crosshatched pattern and (D) micrometer size pillars.

Upon longer irradiation times photodegradation appears to play a major role. In those samples that have been irradiated during longer times (Figure 2(B)) it can be observed that at the interface between exposed/non-exposed areas, a thin region (from 200–300 nm on top up to 2 μm on their base) is formed by crosslinked polymer. According to our observations, in these regions placed at the limit between directly exposed/protected areas the radicals diffused from the exposed areas to the non-exposed producing the crosslinking of the polymer. Taking into account that polystyrene is in a glassy state at room temperature the diffusion is limited and therefore the pattern resolution is rather sharp. This is an interesting aspect since by using this approach different surface patterns with resolutions largely below the resolution provided by the mask employed can be obtained. More precisely, according to the AFM cross-sectional profiles of Figure 3 the half-path width observed is $\sim 1.1 \mu\text{m}$ and the measured radius on top of the patterns $\sim 200\text{--}300 \text{ nm}$.

The radical diffusion towards the non-exposed areas is accompanied by the photodegradation. Thus, as depicted in Figure 2(C) the front crosslinked-degraded moves even below the mask. As a result, rather than open boxes the formation of a crosshatched pattern was observed. More interesting the half-path width for this particular structure is around 1.2 μm as measured by AFM. Finally, photodegradation progresses when using longer irradiations and, as observed in Figure 2(D) only the areas below the crossing points of the mask remained crosslinked. As a result, micrometer size pillars can be produced with a characteristic distance between them provided by the mask employed. In this study, the pillar spacing has been varied between 62 μm and 12.5 μm .

In summary, this approach has, thus, two interesting features: on the one hand, upon larger exposure, degradation of PS occurs as side reaction in those areas directly exposed to the UV irradiation. So that, in principle, it is possible to control the pattern by changing the experimental conditions (time, UV intensity, etc.). Moreover, since crosslinking can be achieved at the exposed-non exposed interface and due to the low radical diffusion in this region the pattern resolution obtained improves the resolution of the mask employed.

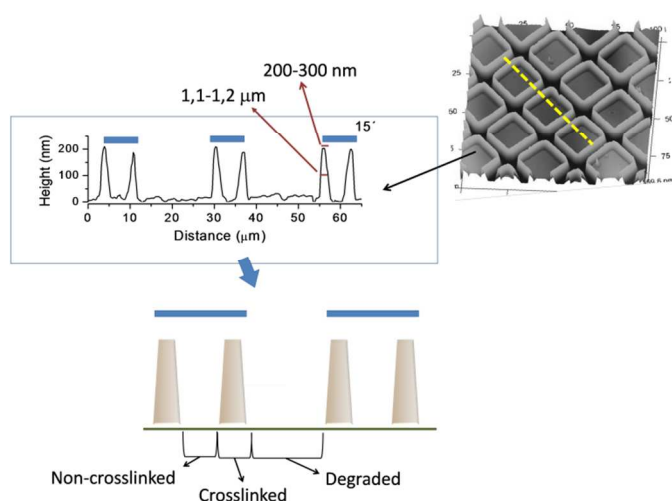


Fig. 3 Top: Cross-sectional profile and 3D AFM image of the open boxes structure with the dimensions on the half-height of the pattern (1.1-1.2 μm) and the diameter on the top of the pattern (~ 200 -300 nm). Down: Model of the structure formed as a consequence of the complete photodegradation of the directly exposed areas and radical diffusion towards the non-exposed regions.

Using these patterned and functional surfaces (taking advantage of the photocrosslinking/photodegradation of PS and simultaneously varying the surface functionality) the formation of bacterial arrays onto polymer surfaces was investigated. The combination of both aspects will allow us to study both the influence of the surface chemical composition that will be achieved by introducing hydrophilic poly(acrylic acid) groups as additives and how can the final polymer pattern direct the bacterial attachment. For that purpose, polystyrene was either employed as unique component or partially combined with the block copolymers. Therefore, the hydrophilicity of the films can be varied depending on the amount of block copolymer introduced within the blend.

Films of the blends were prepared by spin coating from tetrahydrofuran (THF) solutions with a concentration of 30 mg mL^{-1} . Upon UV-light exposure and removal of both degraded and non-crosslinked areas by extensive rinsing, the patterned surface were incubated with *S. aureus* (employed as model bacteria). Bacterial solutions in physiological media were incubated for 1 hour and after thorough wash of the surface the bacteria immobilization was monitored by fluorescence microscopy.

The first series of experiments were carried out using different chemical functionalities in order to find those functional groups that favor the bacterial immobilization. We explored four different systems: (a) polystyrene, (b) polystyrene-*b*-poly(acrylic acid) (PS-*b*-PAA), (c) polystyrene-*b*-poly(L-glutamic acid) (PS-*b*-PGA) and (d) polystyrene-*b*-poly[poly(ethylene glycol) methyl ether methacrylate] (PS-*b*-PEGMA) (Figure 4). The fluorescence images of the films evidenced that by using incubation conditions above depicted two materials, *i.e.* PS-*b*-PAA and PS-*b*-PGA exhibit a large amount of bacterial immobilization onto the patterns created by photocrosslinking (Figure 4b and 4c). These two systems exhibit carboxylic groups at the interface. Carboxylic groups at neutral pH values have negative charge as a consequence of the deprotonation of the acid group. In this situation we would expect that the repulsion between the carboxylic groups and the bacterial membrane would prevent the bacterial adhesion. On the contrary most probably due to the PBS buffer employed with physiological salt concentration the electrostatic repulsion is reduced and permits the bacterial cells to interact with the surface.

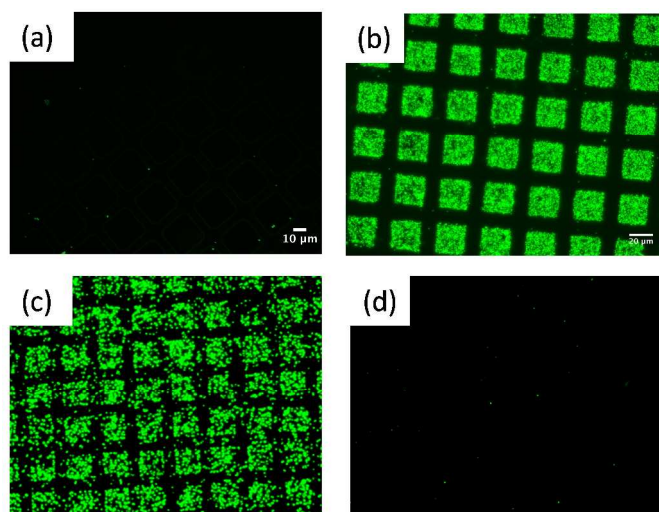


Fig. 4 Fluorescence images of the *S. aureus* adhesion onto square shaped patterns obtained from (a) Polystyrene (PS), (b) PS₂₃-*b*-PAA₁₁, (c) PS₄₉-*b*-PGA₁₇ and (d) PS₄₅-*co*-PEGMA₃₄. (Scale bars: 10 μm).

Upon finding the chemical functionality that favors the bacterial immobilization the following experiments were carried out by using the hydrophobic PS and a variable amount of PS₂₃-*b*-PAA₁₁ block copolymer. On these surfaces, the immobilization of the bacteria was first attempted from a solution at an OD of 1.0 that corresponds to a concentration of about 1.5×10^9 cells mL^{-1} . As a result, whereas the pure polystyrene surfaces required at least 4 h of incubation to evidence the presence of *S. aureus* immobilized at the surface, the incorporation of an amphiphilic block copolymer PS₂₃-*b*-PAA₁₁ significantly promote the bacterial adhesion for the substrates (results not shown here). As a consequence, incubation times as low as 1h resulted in surfaces with a significant bacterial coverage. More interestingly, a gradual increase of the hydrophilicity (as a consequence of the higher amount of block copolymers in the blend) significantly modifies the affinity of the bacteria towards the interface. In Figure 5, are depicted the fluorescence and bright field images of patterned surfaces prepared from PS/PS₂₃-*b*-PAA₁₁ blends with variable amount of PAA. An increase of the surface hydrophilicity is accompanied by an increase of the number of bacteria per motif. More precisely, whereas in the surface with no PAA isolated single bacteria in few of the motifs was observed, an increase to 25 wt% of block copolymer within the blend equally increases the number up to $\sim 23 \pm 3$ bacteria. Further increasing to 50 wt% of block copolymer leads to 32 ± 2 bacteria per square. Finally, by using either 75 wt% of block copolymer or the pure block copolymer the number of bacteria immobilized is close to 41 ± 4 .

As expected, the surface having a larger amount of hydrophilic PAA clearly favors the immobilization of *S. aureus* on the patterned surfaces. In order to extend the concept to other surface structures the crosslinking experiments were carried out using different masks composed of lines, hexagonal or squares shaped features with variable pitch on surfaces formed exclusively by the block copolymer. In Figure 6 are depicted both the modeled surfaces with the different patterns and the resulting fluorescence images of the surfaces upon bacterial immobilization. The fluorescence images clearly evidenced the selective immobilization of a large number of *S. aureus* on the surface areas formed by crosslinked polystyrene whereas almost none bacteria can be observed on the regions where the polymer has been degraded. The results are equally selective in

the different patterned surfaces demonstrating that this is a general approach that can be used to generate different bacteria patterns by simply changing the mask used in the cross-linking process.

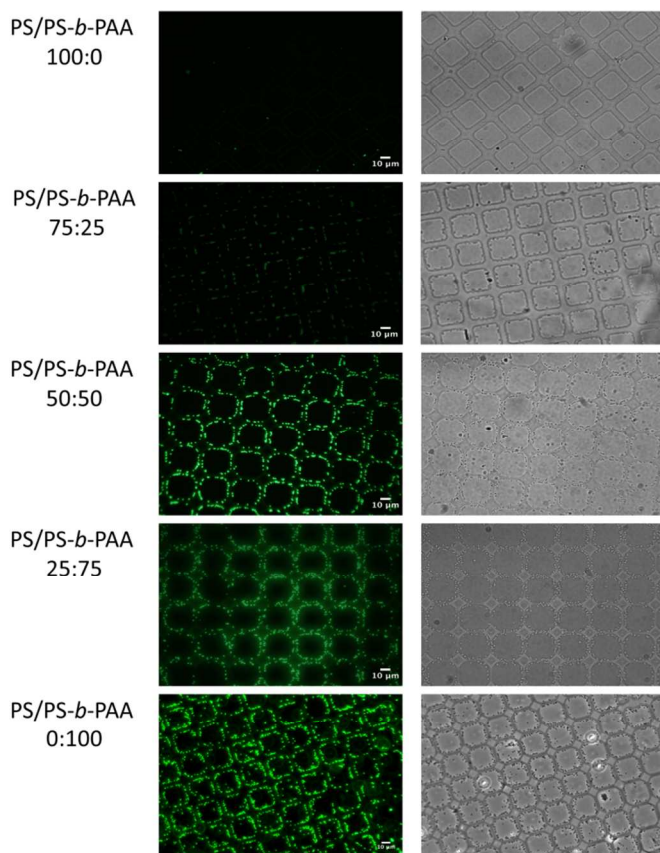


Fig. 5 Fluorescence (left) and bright-field (right) images of the *S. aureus* adhesion onto square shaped patterns obtained from blends of PS and PS₂₃-*b*-PAA₁₁ with variable ratio between pure PS and pure PS₂₃-*b*-PAA₁₁. (Scale bar: 10 μm).

As described above, the use of different masks serve to produce different bacterial arrangements. In addition, the control over the photodegradation/photocrosslinking kinetics allowed us, equally, to obtain different surface patterns. In this concern, the changes of the bacterial distribution on patterned films prepared exclusively with the PS₂₃-*b*-PAA₁₁ block copolymer and a unique mask depending on the pattern created at different irradiation times were evaluated. In **Figure 7** are depicted the fluorescence images of the surfaces having different structural features upon immobilization of the bacterial cells. **Figure 7** shows both the surface pattern and the subsequent bacterial arrays obtained upon immobilization of *S. aureus*. As expected, the photodegradation/photocrosslinking induced variations on the surface topography of the films from cubes (**Fig. 7A**) to pillars (**Fig. 7D**) producing, in addition, two intermediary structures i.e. open boxes (**Fig. 7B**) and crosshatched patterns (**Fig. 7C**). The immobilization occurs in all the cases selectively on the crosslinked areas as a consequence of the affinity between the bacterial cells and the hydrophilic carboxylic acid groups of the poly(acrylic acid) block.

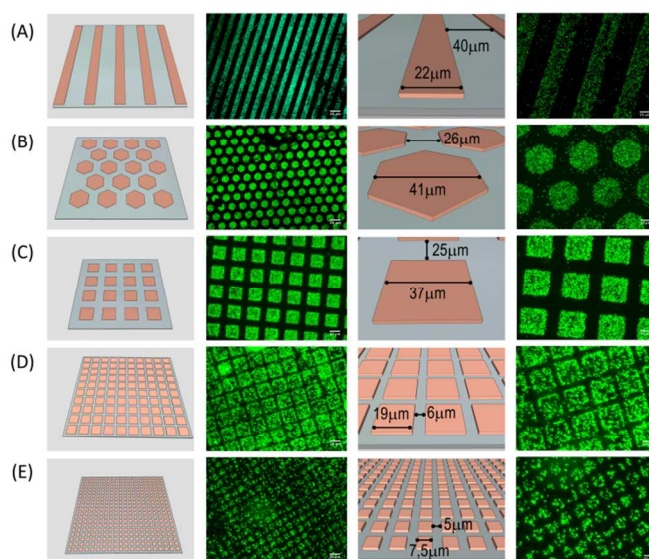


Fig. 6 Bacterial patterns obtained by crosslinking a PS₂₃-*b*-PAA₁₁ block copolymer with UV light (365 nm) and subsequent exposure to a bacterial solution of *S. aureus*. (A) lines (thickness 22 μm), (B) hexagonal arrays (41x51 μm), (C), (D) and (E) square shaped patterns with decreasing pitch from 62 μm, 25 μm to 12.5 μm, respectively. The images in the left panel were acquired using a 20x amplification objective and in the right panel are shown close-up images of the same surfaces using a 40x amplification objective.

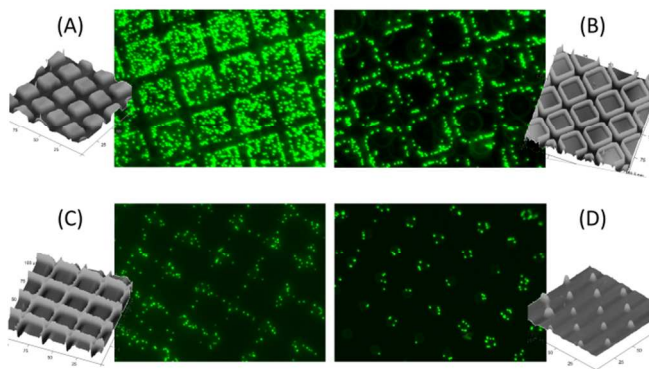


Fig. 7 Variation of the surface pattern and the subsequent bacterial distribution as a function of the treatment employed, i.e. the irradiation times under UV-light. (A) Square shaped distribution (treatment: 15 min UV exposure), (B) open boxes (treatment: 30 min UV exposure) (C) crosshatched pattern (treatment: 1h UV exposure) and (D) pillars (treatment: 2h min UV exposure). Mask: square shaped feature with 25 μm pitch.

In addition to the precise control of the bacterial immobilization of the surface patterns one of the main objectives of this study is the immobilization of *S. aureus* cells to form single cell arrays. Previously reported literature focused on other types of bacteria such as *Escherichia coli*^{11, 35} or *Pseudomonas aeruginosa*³² while *S. aureus* in spite of their major role in multiple infection diseases has been somehow neglected. This is probably due to the large tendency of *S. aureus* to form aggregates that difficult their isolation and immobilization as single cells.^{43, 56} In order to immobilize *S. aureus* as single entities the surface patterns created by crosslinking at the

exposed-non exposed areas were employed. In these cases, due to the high resolution of the pattern ($1\mu\text{m}$ and below) which is even below the dimension of the *S. aureus* diameter ($\sim 1\mu\text{m}$) we expect to anchor single cells on top of the micrometer/submicrometer size pattern. The resulting bacterial arrays obtained are depicted in **Figure 8**. On the top [(A), (B)] are depicted the surface patterns obtained with short UV-exposures and subsequent bacterial immobilization monitored by fluorescence microscopy (central panels) and by STEM (right panels). On the bottom [(C), (D) and (E)] the bacterial arrays on different surface patterns generated by photocrosslinking on the edge (shadow-illuminated) areas of the mask. The A and B panels demonstrated the capability of the surface to immobilize *S. aureus* in different shapes. However, as has been already mentioned the bacteria are distributed forming large clusters on top of the pattern. On the contrary, the immobilization of *S. aureus* on the submicrometer patterns exhibits a different behavior. As can be observed in **Figure 8 (C)** and (D) the bacteria can be aligned on top of the patterned surface as a consequence of the large affinity between the bacteria and the hydrophilic PAA groups. As a consequence either corrals or lines of bacteria can be easily constructed. More interestingly, larger irradiation times using a square shaped mask leads to micrometer size pillars in which a single bacteria can be immobilized (**Figure 8(E inset)**).

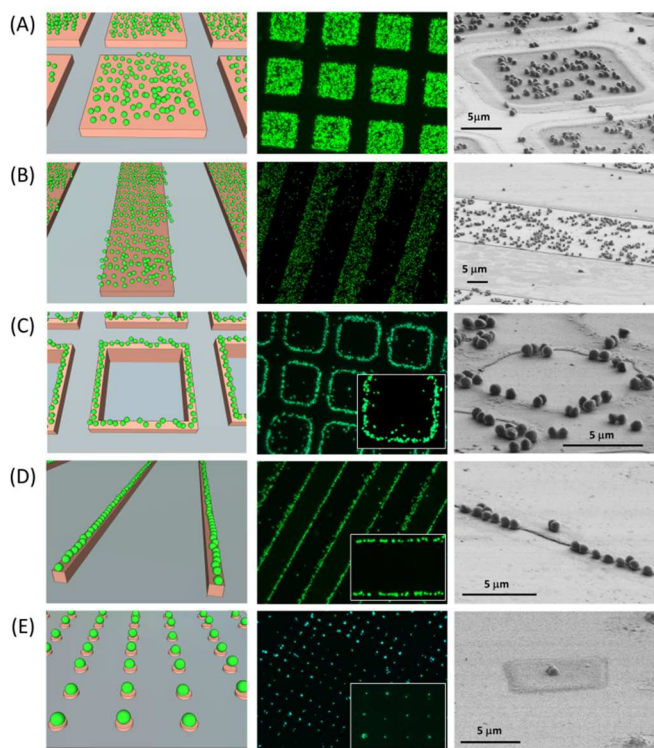


Fig. 8 Surface bacterial patterns generated using short irradiation times (panels, A and B) and upon longer irradiation where the directly exposed areas have been photodegraded (panels C, D and E). Masks employed (A and C) squares with a pitch of $25\mu\text{m}$, (B and D) lines with a width of $22\mu\text{m}$ and (E) squares with a pitch of $12.5\mu\text{m}$. The fluorescence microscopy (central panels) and STEM (right panels) images show the selective immobilization of fluorescent *S. aureus* bacteria. C, D and E included an inset with a close-up image showing individual bacteria immobilization.

In summary, the simple approach depicted herein allows the formation of a large variety of surface patterns depending on the mask employed and the chemical composition of the polymer blend employed. Among others, as demonstrated herein this approach can be employed for the selective adhesion both of single bacteria in pillars and single bacteria alignment. One can envision many potential uses of these platforms. For example, the isolation of cluster growing bacteria can be applied for individual identification and diagnosis. The isolated positioning at the surface might be critical in the cases that are many variants of the same bacterial strain but only some associated with disease, such as in the antibiotic-resistant infections. Another broad field of application of these single cell array platforms concerns the study of different biological processes at the single cell level in a large bacteria population. Those studies have great relevance, for instance, to unravel biological stochastic processes, including gene expression because it has been shown that not even genetically identical cells behave the same.⁵⁷⁻⁶⁰

Conclusions

The formation of bacterial surface arrays by using a photolithographic approach having some particular features has been described. First, the methodology employed permitted the incorporation of functional groups able to modify the affinity between the bacteria and the surface. Thus, the incorporation of hydrophilic segments, i.e. PAA favors the bacterial immobilization. Second, the amount of hydrophilic segment introduced can be finely tuned by preparing blends of the block copolymer and linear polystyrene. This unique feature has been employed to determine the role of the surface hydrophilicity on the adhesion of *S. aureus* onto the different surface patterns. More interestingly, the photolithographic approach employed produced different patterns not only depending on the mask employed but also depending on the experimental conditions applied. As a consequence, by using standard equipment without the requirement of expensive fine focalization settings lead to the formation of patterns with nanoscale resolution. The latter has been found to be crucial in order to prepare arrays of isolated bacteria as has been evidenced by using *S. aureus*. It has to be pointed out that the use of *S. aureus* has been up to know somehow neglected mainly due to their aggregation.

Acknowledgements

The authors gratefully acknowledge support from the Consejo Superior de Investigaciones Científicas (CSIC). Equally, this work was financially supported by the Ministerio de Economía y Competitividad (MINECO) through MAT2011-22861, MAT2013-47902-C2-1-R (JRH), and BIO2012-34835 (ALC). M. Palacios thanks the Ministerio de Education for the FPU fellowship. This research is funded in part by the European Commission International Reintegration Grant (IRG-246688) (ALC) and AMAROUT-COFUND Europe Programme (ALC).

Notes and references

^a Department of Chemistry and Properties of Polymers, Instituto de Ciencia y Tecnología de Polímeros, (ICTP-CSIC), Juan de la Cierva 3, 28006-Madrid, Spain.

* To whom correspondence should be addressed. E-mail: ogarcia@ictp.csic.es and rodriguez@ictp.csic.es

- ^b Instituto Madrileño de Estudios Avanzados en Nanociencia (IMDEA-Nanociencia), Cantoblanco, 28049 Madrid, Spain & CNB-CSIC-IMDEA Nanociencia Associated Unit "Unidad de Nanobiotecnología".
- D. Alves and M. O. Pereira, *Biofouling*, 2014, 30, 483-499.
 - J. Hasan, R. J. Crawford and E. P. Lvanova, *Trends in Biotechnology*, 2013, 31, 31-40.
 - V. Nandakumar, S. Chittaranjan, V. M. Kurian and M. Doble, *Polymer Journal*, 2013, 45, 137-152.
 - S. T. Reddy, K. K. Chung, C. J. McDaniel, R. O. Darouiche, J. Landman and A. B. Brennan, *Journal of Endourology*, 2011, 25, 1547-1552.
 - K. Salaita, Y. Wang and C. A. Mirkin, *Nature Nanotechnology*, 2007, 2, 145-155.
 - Y.-K. Kim, S.-R. Ryoo, S.-J. Kwack and D.-H. Min, *Angewandte Chemie-International Edition*, 2009, 48, 3507-3511.
 - A. I. Hochbaum and J. Aizenberg, *Nano Letters*, 2010, 10, 3717-3721.
 - D. D. Doorneweerd, W. A. Henne, R. G. Reifengerger and P. S. Low, *Langmuir*, 2010, 26, 15424-15429.
 - F. Bai, R. W. Branch, D. V. Nicolau, Jr., T. Pilizota, B. C. Steel, P. K. Maini and R. M. Berry, *Science*, 2010, 327, 685-689.
 - S. Rozhok, C. K. F. Shen, P. L. H. Littler, Z. F. Fan, C. Liu, C. A. Mirkin and R. C. Holz, *Small*, 2005, 1, 445-451.
 - S. Rozhok, Z. Fan, D. Nyamjav, C. Liu, C. A. Mirkin and R. C. Holz, *Langmuir*, 2006, 22, 11251-11254.
 - B. Rowan, M. A. Wheeler and R. M. Crooks, *Langmuir*, 2002, 18, 9914-9917.
 - N. R. Thirumalapura, R. J. Morton, A. Ramachandran and J. R. Malayer, *Journal of Immunological Methods*, 2005, 298, 73-81.
 - N. R. Thirumalapura, A. Ramachandran, R. J. Morton and J. R. Malayer, *Journal of Immunological Methods*, 2006, 309, 48-54.
 - C.-H. Choi, J.-H. Lee, T.-S. Hwang, C.-S. Lee, Y.-G. Kim, Y.-H. Yang and K. M. Huh, *Macromolecular Research*, 2010, 18, 254-259.
 - Y. Kuang, I. Biran and D. R. Walt, *Analytical Chemistry*, 2004, 76, 2902-2909.
 - Z. Suo, R. Avci, X. Yang and D. W. Pascual, *Langmuir*, 2008, 24, 4161-4167.
 - I. Biran, D. M. Rissin, E. Z. Ron and D. R. Walt, *Analytical Biochemistry*, 2003, 315, 106-113.
 - T. K. Van Dyk, E. J. DeRose and G. E. Gonye, *Journal of Bacteriology*, 2001, 183, 5496-5505.
 - M. B. Miller and B. L. Bassler, *Annual Review of Microbiology*, 2001, 55, 165-199.
 - S. Raina, D. De Vizio, M. Odell, M. Clements, S. Vanhulle and T. Keshavarz, *Biotechnology and Applied Biochemistry*, 2009, 54, 65-84.
 - B. A. Hense, C. Kuttler, J. Mueller, M. Rothballer, A. Hartmann and J.-U. Kreft, *Nature Reviews Microbiology*, 2007, 5, 230-239.
 - C. M. Thomas and K. M. Nielsen, *Nature Reviews Microbiology*, 2005, 3, 711-721.
 - S. J. Sorensen, M. Bailey, L. H. Hansen, N. Kroer and S. Wuerzt, *Nature Reviews Microbiology*, 2005, 3, 700-710.
 - B. V. Merkey, L. A. Lardon, J. M. Seoane, J.-U. Kreft and B. F. Smets, *Environmental Microbiology*, 2011, 13, 2435-2452.
 - A. Cerf, J.-C. Cau and C. Vieu, *Colloids and Surfaces B: Biointerfaces*, 2008, 65, 285-291.
 - D. B. Weibel, A. Lee, M. Mayer, S. F. Brady, D. Bruzewicz, J. Yang, W. R. DiLuzio, J. Clardy and G. M. Whitesides, *Langmuir*, 2005, 21, 6436-6442.
 - Y.-j. Xie, H.-y. Yu, S.-y. Wang and Z.-k. Xu, *Journal of Environmental Sciences-China*, 2007, 19, 1461-1465.
 - C. M. Costello, J.-U. Kreft, C. M. Thomas, D. M. Hammes, P. Bao, S. D. Evans and P. M. Mendes, *Soft Matter*, 2012, 8, 9147-9155.
 - K. Y. Suh, A. Khademhosseini, P. J. Yoo and R. Langer, *Biomedical Microdevices*, 2004, 6, 223-229.
 - P. Krsko, J. B. Kaplan and M. Libera, *Acta Biomaterialia*, 2009, 5, 589-596.
 - D. Nyamjav, S. Rozhok and R. C. Holz, *Nanotechnology*, 2010, 21, 6.
 - P. Kim, A. Epstein, M. Khan, L. Zarzar, D. Lipomi, G. Whitesides and J. Aizenberg, *Nano letters*, 2012, 12, 527-533.
 - W. G. Koh, A. Revzin, A. Simonian, T. Reeves and M. Pishko, *Biomedical Microdevices*, 2003, 5, 11-19.
 - N. J. Lawrence, J. M. Wells-Kingsbury, M. M. Ihrig, T. E. Fangman, F. Namavar and C. L. Cheung, *Langmuir*, 2012, 28, 4301-4308.
 - T. Xu, S. Petridou, E. H. Lee, E. A. Roth, N. R. Vyavahare, J. J. Hickman and T. Boland, *Biotechnology and Bioengineering*, 2004, 85, 29-33.
 - K. Kim, B. U. Lee, G. B. Hwang, J. H. Lee and S. Kim, *Analytical Chemistry*, 2010, 82, 2109-2112.
 - J. Kim, Y.-H. Shin, S.-H. Yun, D.-S. Choi, J.-H. Nam, S. R. Kim, S.-K. Moon, B. H. Chung, J.-H. Lee, J.-H. Kim, K.-Y. Kim, K.-M. Kim and J.-H. Lim, *Journal of the American Chemical Society*, 2012, 134, 16500-16503.
 - L. Kailas, E. C. Ratcliffe, E. J. Hayhurst, M. G. Walker, S. J. Foster and J. K. Hobbs, *Ultramicroscopy*, 2009, 109, 775-780.
 - S. Kasas and A. Ika, *Biophysical Journal*, 1995, 68, 1678-1680.
 - A. Beaussart, S. El-Kirat-Chatel, P. Herman, D. Alsteens, J. Mahillon, P. Hols and Yves F. Dufrêne, *Biophysical Journal*, 104, 1886-1892.
 - K. Anselme, P. Davidson, A. M. Popa, M. Giazon, M. Liley and L. Ploux, *Acta Biomaterialia*, 2010, 6, 3824-3846.
 - T. Koyama, M. Yamada and M. Matsuhashi, *Journal of Bacteriology*, 1977, 129, 1518-1523.
 - N. Ktari, P. Poncet, H. Sénéchal, L. Malaquin, F. Kanoufi and C. Combellas, *Langmuir*, 2010, 26, 17348-17356.
 - W. Pflöging, M. Bruns, M. Przybylski, A. Welle and S. Wilson, 2008.
 - W. H. Kuo, M. J. Wang, C. W. Chang, T. C. Wei, J. Y. Lai, W. B. Tsai and C. Lee, *Journal of Materials Chemistry*, 2012, 22, 9991-9999.
 - M. R. Dusseiller, D. Schlaepfer, M. Koch, R. Kroschewski and M. Textor, *Biomaterials*, 2005, 26, 5917-5925.
 - A. S. De León, A. Del Campo, M. Fernández-García, J. Rodríguez-Hernández and A. Muñoz-Bonilla, *Langmuir*, 2012, 28, 9778-9787.
 - Y. Zheng, Y. Kubowaki, M. Kashiwagi and K. Miyazaki, *Journal of Mechanical Science and Technology*, 2011, 25, 33-36.
 - P. Vakuliuk, A. Burban, V. Konovalova, M. Bryk, M. Vortman, N. Klymenko and V. Shevchenko, *Desalination*, 2009, 235, 160-169.
 - M. Ghezzi, S. C. Thickett and C. Neto, *Langmuir*, 2012, 28, 10147-10151.
 - G. T. Carroll, N. J. Turro and J. T. Koberstein, *Journal of Colloid and Interface Science*, 2010, 351, 556-560.
 - I. W. Moran, J. R. Ell and K. R. Carter, *Small*, 2011, 7, 2669-2674.
 - M. Palacios, O. Garcia and J. Rodriguez-Hernandez, *Langmuir*, 2013, 29, 2756-2763.
 - M. Palacios-Cuesta, A. L. Cortajarena, O. Garcia and J. Rodriguez-Hernandez, *Biomacromolecules*, 2013, 14, 3147-3154.
 - D. H. Bergey and J. G. Holt, *Bergey's Manual of Determinative Bacteriology*, Williams & Wilkins, 1994.
 - M. B. Elowitz, A. J. Levine, E. D. Siggia and P. S. Swain, *Science*, 2002, 297, 1183-1186.
 - A. Raj and A. van Oudenaarden, *Cell*, 2008, 135, 216-226.
 - B. Munsky, G. Neuert and A. van Oudenaarden, *Science*, 2012, 336, 183-187.
 - A. Raj, S. A. Rifkin, E. Andersen and A. van Oudenaarden, *Nature*, 2010, 463, 913-U984.